Electronic Supplementary Information

Post-polymerization modification of polybenzoxazines by boronic acids supported by B–N interactions

Yuki Tsukamoto, Jumpei Kida, Daisuke Aoki and Hideyuki Otsuka*

Department of Chemical Science and Engineering, Tokyo Institute of Technology,

2-12-1 Ookayama, Meguro-ku, Tokyo 152-8550, Japan

*Corresponding author: Hideyuki Otsuka (Email: otsuka@mac.titech.ac.jp)

Materials and instruments

1,4-Dioxane was stored over molecular sieves 4Å (MS 4Å) under N_2. **BHBA-p**, ***p*C-p** and **B-p** were synthesized according to previously reported procedures.[1,2] Unless otherwise noted, other reagents and solvents used for this study were commercially available and used as supplied. ^{1}H nuclear magnetic resonance (NMR) spectra and diffusion-ordered spectroscopy (DOSY) spectra were recorded on a Bruker topspin AVANCE III HD500 spectrometer, using $CDCl_3$ or hexadeuterodimethyl sulfoxide (DMSO-d_6) as solvents. Unless otherwise mentioned, the spectra were taken at room temperature. In NMR spectra, the signals of residual undeuterated solvent were used as the internal standard. Fourier transform infrared (FT-IR) spectra were recorded on a JASCO FT/IR-4100 spectrometer. Differential scanning calorimetry (DSC) measurements were carried out on a SHIMADZU DSC-60A Plus with a heating rate of 10 °C/min. Fluorescence spectra were measured on a JASCO FP-6600 spectrofluorometer. Thermogravimetric analysis (TGA) measurements were performed on a SHIMADZU DTG-60 in a nitrogen stream of 50 ml min^{-1} at a heating rate of 10 °C min^{-1}, ranging from 30 to 600 °C. Gel permeation chromatography (GPC) was performed in *N*,*N*-dimethylformamide (DMF) at 40 °C using a JASCO ChromNAV Lite system equipped a guard column (TOSOH TSK guard column Super H-L), three columns (TOSOH TSK gel SuperH 6000, 4000, and 2500), a differential refractive index (RI) detector system. The number average molecular weight (M_n) and polydispersity index (M_w/M_n) of the polymers were calculated on the basis of a polystyrene calibration.

Model reactions of BHBA-p and boronic acids

BHBA-p (5.00 mg, 16.7 μmol) and equimolar amount of **MPBA** were dissolved in 500 μL of $CDCl_3$ in a glass vial respectively, and transferred to an NMR test tube. ^{1}H NMR spectra of solution were measured at 25 °C. All model reactions using anthraceneboronic acid isomers were conducted in the same manner in DMSO-d_6.

Synthesis of BHBA-p–MPBA

BHBA-p (100.0 mg, 0.334 mmol) and **MPBA** (45.4 mg, 0.334 mmol) were dissolved in 2.0 mL of $CHCl_3$ in a glass vial. The mixture was stirred at room temperature for 24 h, then the solvent was evaporated. The mixture was purified by silica-gel column chromatography (hexane/dichloromethane = 1/1, v/v) to yield white solid (130 mg, 97%). ^{1}H NMR (500 MHz, $CDCl_3$): δ/ppm 0.81 (t, J = 7.3 Hz, 3H), 1.57 (sext, J = 7.8 Hz, 2H), 2.26 (s, 6H), 2.29 (s, 3H), 2.85 (t, J = 8.5 Hz, 2H), 3.86 (d, J = 14.9 Hz, 2H), 4.14 (d, J = 14.9 Hz, 2H), 6.70 (s, 2H), 6.91 (d, J = 8.3 Hz, 2H), 7.03 (m, 4H), 7.44 (d, J = 7.9 Hz, 2H); ^{13}C NMR (125 MHz, $CDCl_3$): δ/ppm 11.43, 14.24, 20.62, 21.44, 53.67, 55.16, 116.39, 119.12, 127.35, 128.13, 128.36, 130.36, 133.43, 137.25, 151.70; FT-IR (NaCl): $\tilde{\nu}$/cm^{-1} 3008, 2974, 2922, 2875, 1616, 1585, 1502, 1450, 1363, 1288, 1259, 1234, 1186, 1151, 1128, 1057, 1024, 985, 933, 858, 820, 756, 714, 665, 575; HRMS (FAB): 422.2269 $[M+Na]^+$, calculated for $C_{26}H_{30}NO_2BNa$ $[M+Na]^+$: 422.2267.

Synthesis of BHBA-p–2-AnBA

BHBA-p (94.4 mg, 0.315 mmol) and **2-AnBA** (70.0 mg, 0.315 mmol) were mixed in 5.0 mL of THF in a glass vial. The mixture was stirred at room temperature for 24 h, then the solvent was evaporated. The mixture was purified by silica-gel column chromatography (hexane/dichloromethane = 2/1, v/v) to yield white solid (95.4 mg, 62%). ^{1}H NMR (500 MHz, DMSO-d_6): δ/ppm 0.71 (t, J = 7.3 Hz, 3H), 1.61 (sext, J = 7.8 Hz, 2H), 2.25 (s, 6H), 2.80 (t, J = 8.5 Hz, 2H), 4.04 (d, J = 15.7 Hz, 2H), 4.18 (d, J = 15.7 Hz, 2H), 6.81 (d, J = 8.2 Hz, 2H), 6.90 (s, 2H), 7.06 (m, 2H), 7.45 (m, 2H), 7.56 (d, J = 8.8 Hz, 1H), 7.90 (d, J = 8.7 Hz, 1H), 8.04 (m, 2H), 8.09 (s, 1H), 8.36 (s, 1H), 8.45 (s, 1H); ^{13}C NMR (125 MHz, DMSO-d_6): δ/ppm 11.12, 13.81, 20.17, 52.83, 55.38, 117.09, 117.86, 125.02, 125.16, 125.20, 125.93, 126.04, 127.65, 127.79, 127.85, 128.08, 129.87, 130.32, 130.98, 131.07, 131.19, 132.57, 151.13; FT-IR (NaCl): ν~/cm^{-1} 3008, 2976, 2877, 1734, 1618, 1585, 1502, 1452, 1423, 1362, 1288, 1267, 1232, 1157, 1128, 1059, 1001, 914, 874, 820, 756, 667, 544; HRMS (ESI): 508.2416 $[M+Na]^+$, calculated for $C_{33}H_{32}NO_2BNa$ $[M+Na]^+$: 508.2418.

Determination of hydrolysis equilibrium constant of BHBA-p–MPBA and dioxazaborocane at 25 °C (taking BHBA-p–MPBA as an example)

As reported by Jing's group, the hydrolysis equilibrium constant (K_{eq}) for **BHBA-p**–**MPBA** was determined by using ^{1}H NMR spectrum based on the following equation:[3]

$$K_{eq} = \frac{k_1}{k_{-1}} = \frac{[MPBA][BHBA\text{–}p]}{[BHBA\text{–}p - MPBA][H_2O]^2}$$

Determination of binding constant

The binding constant (K_a) for BHBA and boronic acid was determined by using ^{1}H NMR spectrum based on the following equation:[4]

$$K_a = \frac{I_{DOAB}}{I_{BHBA}\left(n_{BA} - \frac{I_{DOAB}}{I_{BHBA} + I_{DOAB}} n_{BHBA}\right)}$$

where I_{DOAB} is the integral value of protons in DOAB; I_{BHBA} is the integral value of protons in BHBA; n_{BA} is the initial molar concentration of the boronic acid; n_{BHBA} is the initial molar concentration of the BHBA.

Synthesis of linear polybenzoxazine (P*p*C-p)[2]

Scheme S1. Synthesis of linear polybenzoxazine (**P*p*C-p**).

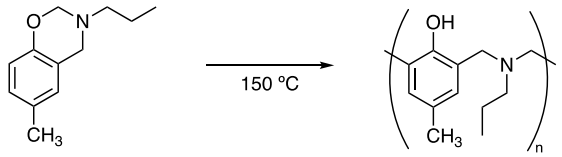

***p*C-p** **P*p*C-p**

***p*C-p** (5.12 g, 26.8 mmol) was degassed by freeze-pump-thaw method for three times before undergoing thermally induced polymerization at 150 °C for 6 days under a nitrogen atmosphere. The reaction mixture was dissolved in chloroform and reprecipitated into methanol. After drying under vacuum, **P*p*C-p** was obtained as yellow solid (4.22 g, 82%). M_n = 2,200, M_w/M_n = 1.41. The complete polymerization of **P*p*C-p** was confirmed by the lack of exothermic peaks in the DSC profile (Fig. S2). This compound has already appeared in the literature,[2] and its spectral and analytical data are in good agreement with those reported. Accordingly, ^{1}H NMR data and FT-IR data are provided here. ^{1}H NMR (500 MHz, $CDCl_3$): δ/ppm 0.70–0.88 (m, 3H), 1.46–1.67 (m, 2H), 2.17–2.23 (m, 3H), 2.32–2.52 (m, 2H), 3.57–3.78 (m, 4H), 6.50–7.02 (m, 2H); FT-IR (NaCl): $\tilde{\nu}$/cm^{-1} 2961, 2932, 2872, 1633, 1611, 1480, 1381, 1297, 1254, 1156, 1117, 1061, 986, 864, 776, 573.

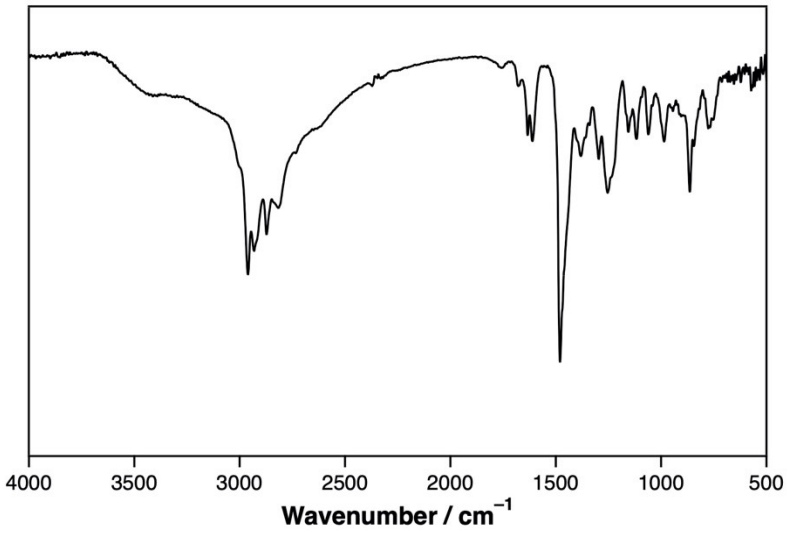

Fig. S1. FT-IR spectrum of **P*p*C-p** (NaCl).

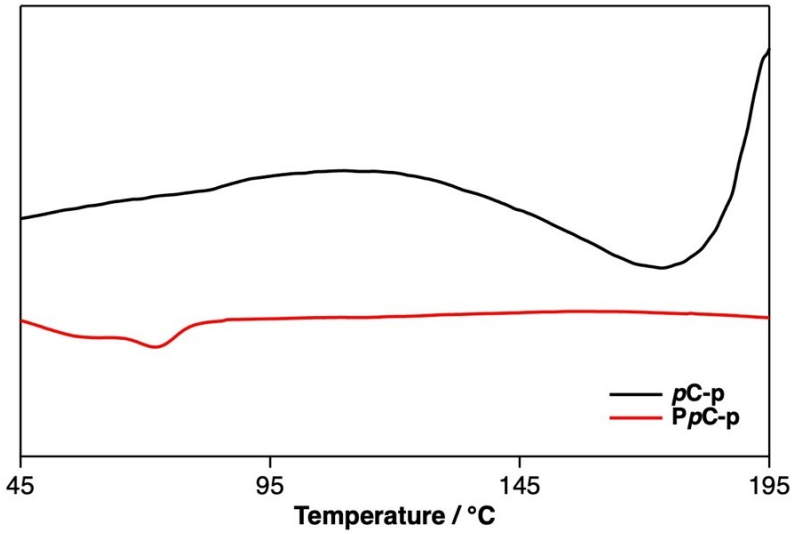

Fig. S2. DSC profiles of ***p*C-p** (black) and **P*p*C-p** (red) at a heating rate of 10 °C/min.

Reaction of P*p*C-p with boronic acid

P*p*C-p (5.00 mg with approx. 13.1 μmol of BHBA units) and **MPBA** (1.78 mg, 13.0 μmol) were mixed in 500 μL of in $CDCl_3$ in a glass vial and transferred to an NMR test tube. ^{1}H NMR spectrum and DOSY spectrum were recorded after to assess the generation of the adduct (**P*p*C-p**–**MPBA**). ^{1}H NMR (500 MHz, $CDCl_3$): δ/ppm 0.79 (br, 3H), 1.53 (br, 2H), 1.97–2.57 (m, 11H), 0.79 (br, 3H), 6.30–8.17 (m, 8H).

Synthesis of (hexane-1,6-diylbis(oxy))bis(4-bromobenzene) (1)[5]

Scheme S2. Synthesis of **1**.

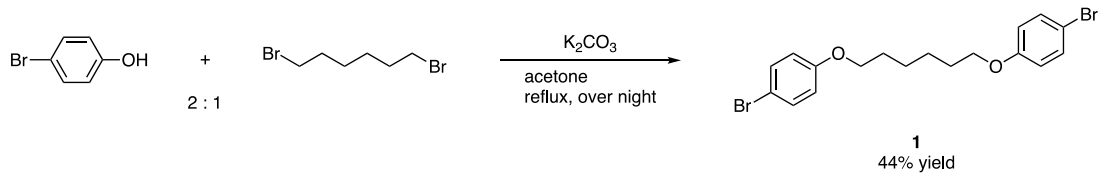

4-Bromophenol (1.00 g, 5.78 mmol), 1,6-dibromohexane (0.705 g, 2.89 mmol), and K_2CO_3 (2.90 g, 21.0 mmol) were added to acetone (25 mL) and the mixture was heated under reflux overnight. The reaction mixture was cooled to room temperature and the white solid was filtered off, then washed with acetone. The organic layer was evaporated under reduced pressure. The mixture was purified by silica-gel column chromatography (hexane/ethyl acetate = 40/1, v/v) to yield compound **1** as white solid (0.545 g, 44%). ^{1}H NMR (500 MHz, $CDCl_3$): δ/ppm 1.52 (quin, J = 3.6 Hz, 4H), 1.80 (quin, J = 6.8 Hz, 4H), 3.93 (t, J = 6.4 Hz, 4H), 6.76 (d, J = 8.9 Hz, 4H), 7.36 (d, J = 8.9 Hz, 4H); ^{13}C NMR (125 MHz, $CDCl_3$): δ/ppm 25.93, 29.22, 68.16, 112.77, 116.41, 132.34, 158.30; FT-IR (KBr): $\tilde{\nu}$/cm^{-1} 3091, 2941, 2866, 2060, 1884, 1589, 1491, 1473, 1400, 1288, 1248, 1174, 1105, 1076, 1022, 1001, 829, 808, 733, 638, 507, 467, 428; HRMS (EI): 425.9838 $[M]^+$, calculated for $C_{18}H_{20}Br_2O_2$ $[M]^+$: 425.9830.

Synthesis of diBA[5]

Scheme S3. Synthesis of **diBA**.

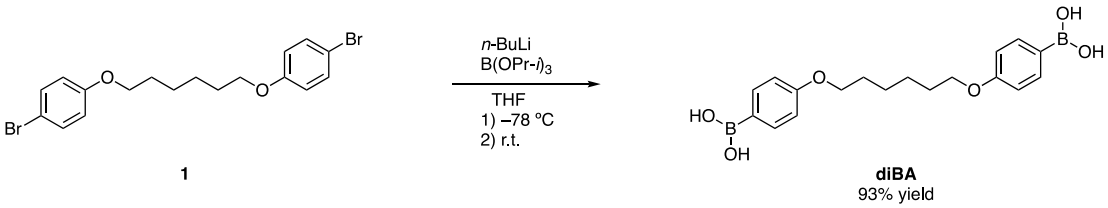

A solution of compound **1** (0.500 g, 1.17 mmol) in 10 mL of THF was cooled to −78 °C. *n*-BuLi in hexane (1.6 mol/L, 1.61 mL, 2.57 mmol) was slowly added and stirred for an additional 30 min before triisopropylborate (0.483 g, 0.589 mL, 2.57 mmol) was added. The reaction mixture was then left to warm up to r.t. and stirred overnight. Aqueous HCl (1 M, 3 mL) was added to quench the reaction and the solvent was removed under reduced pressure. Obtained solid was washed with water (8 mL × 3) and 1:1 hexane/DCM mixture (8 mL × 2) and dried under vacuum. **diBA** was obtained as a white solid (0.393 g, 93%). ^{1}H NMR (500 MHz, DMSO-d_6): δ/ppm 1.46 (m, 4H), 1.73 (m, 4H), 3.97 (t, J = 6.4 Hz, 4H), 6.87 (d, J = 8.4 Hz, 4H), 7.72 (d, J = 8.4 Hz, 4H), 7.82 (br s, 4H); ^{13}C NMR (125 MHz, DMSO-d_6): δ/ppm 25.36, 28.68, 67.11, 113.42, 135.86, 160.40 (The carbon signal of the C–B was not observed.); FT-IR (KBr): $\tilde{\nu}$/cm^{-1} 3339, 2942, 1606, 1362, 1249, 1178, 1107, 1003, 827, 652; HRMS (ESI): 393.1470 $[M+Cl]^-$, calculated for $C_{18}H_{24}B_2O_6Cl$ $[M+Cl]^-$: 393.1453.

Gelation of P*p*C-p

P*p*C-p (0.268 g with approx. 0.700 mmol of BHBA units) and **diBA** (0.107 g, 0.30 mmol) were mixed in 0.60 mL of DMF in a glass vial. Then, approximately 160 mg of molecular sieves 4Å was added to the solution, and gelation was observed 24 hours later.

Synthesis of cross-linked polybenzoxazine (PB-p)

Scheme S4. Synthesis of **PB-p**.

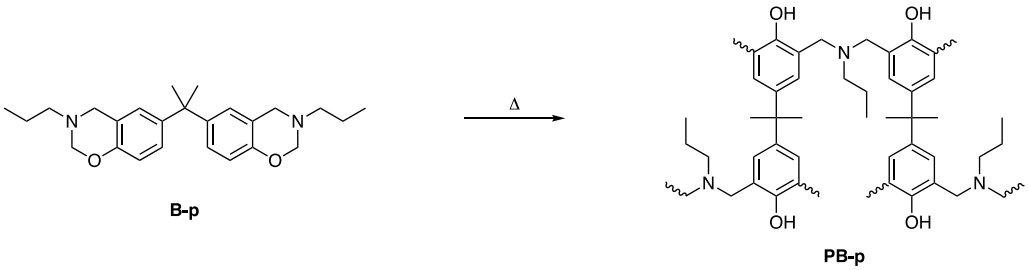

B-p was heated at 150 °C under a nitrogen atmosphere for 24 h on a round Teflon mold (ϕ = 1.5 cm). FT-IR (KBr): $\tilde{\nu}$/cm^{-1} 2962, 2871, 1676, 1608, 1481, 1383, 1259, 1228, 1190, 1142, 1119, 1055, 976, 935, 822, 777, 748, 669, 611, 530. The DSC profiles of **B-p** and **PB-p** were as shown in Fig. S4.

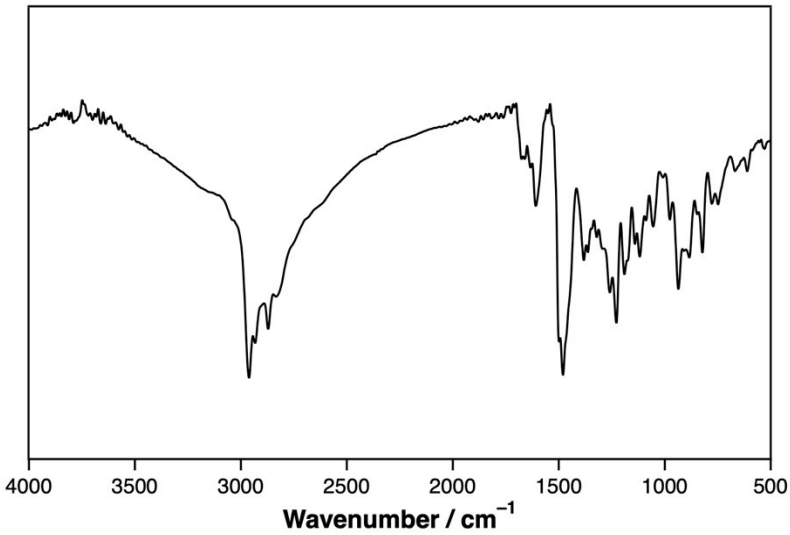

Fig. S3. FT-IR spectrum of **PB-p** (KBr).

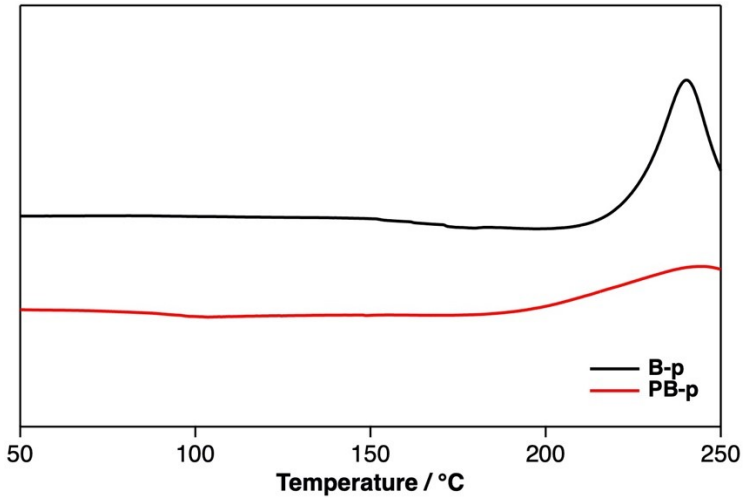

Fig. S4. DSC profiles of **B-p** (black) and **PB-p** (red) at a heating rate of 10 °C/min.

Modification of PB-p by fluorescent boronic acid

Crushed samples of **PB-p** were immersed in 1 mL of tetrahydrofuran (THF) solution of an anthraceneboronic acid (**2-AnBA** or **9-AnBA**) (5.0×10^{-2} M) under a nitrogen atmosphere for 24 hours. The samples were then washed with THF and dried in the ambient condition. Fluorescence spectra of the treated sample were measured to evaluate the incorporation of boronic acid into **PB-p**. In the case of circular sample of the **PB-p**, modification was conducted by immersing in 1,4-dioxane/THF (= 2/1) solution of anthraceneboronic acid (2.0×10^{-2} M) under a nitrogen atmosphere for 48 hours.

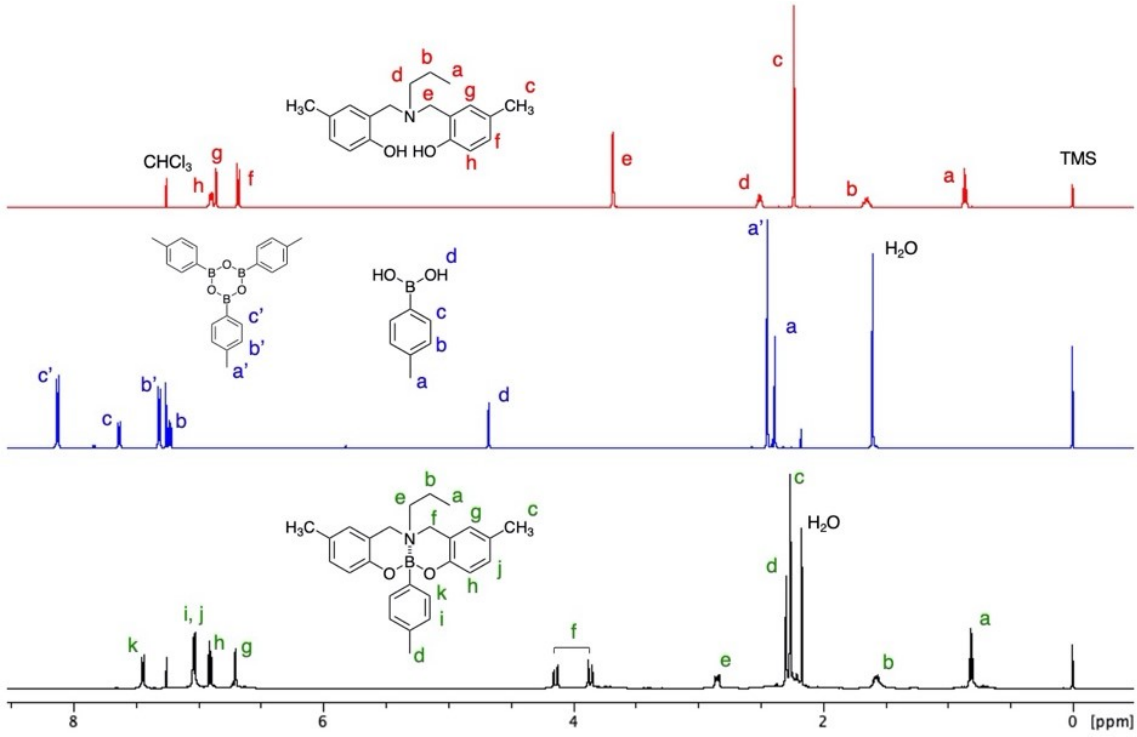

Fig. S5. ^{1}H NMR spectra of the mixture of equimolar **BHBA-p** and **MPBA** (black), **MPBA** (blue), and **BHBA-p** (red) ($CDCl_3$, 500 MHz).

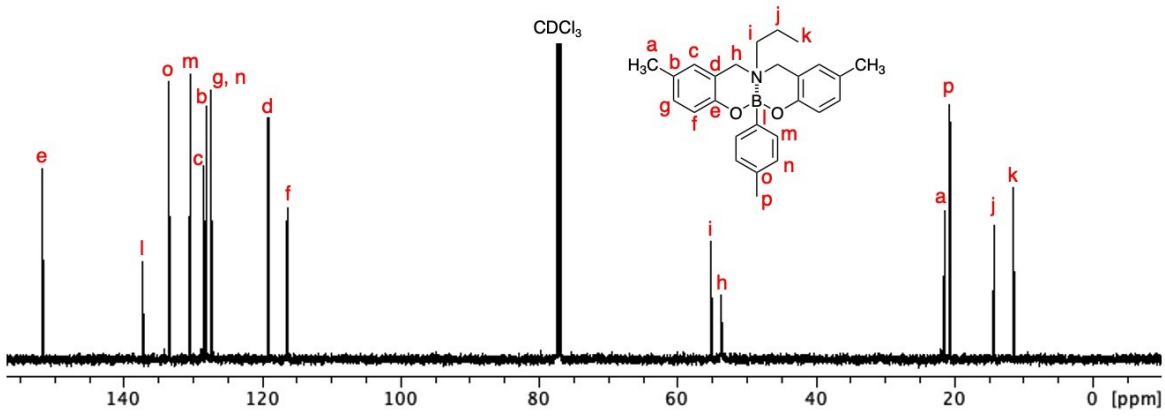

Fig. S6. ^{13}C NMR spectrum of **BHBA-p**–**MPBA** ($CDCl_3$, 125 MHz).

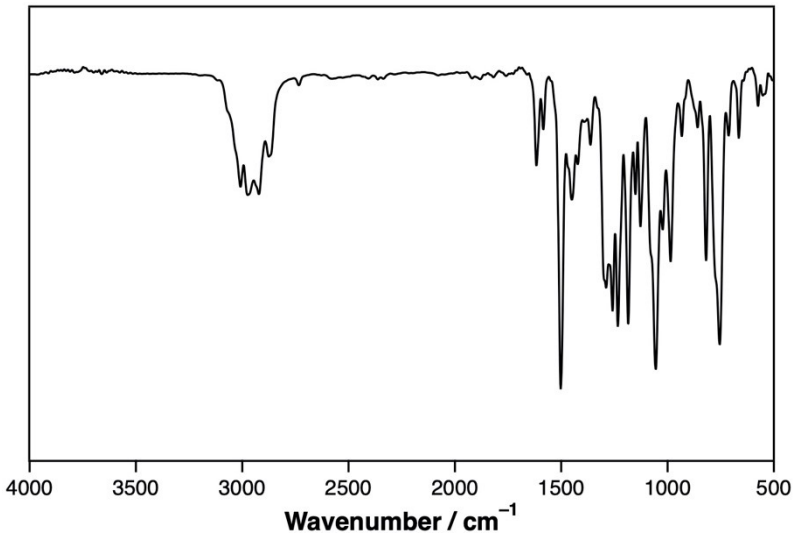

Fig. S7. FT-IR spectrum of **BHBA-p**–**MPBA** (NaCl).

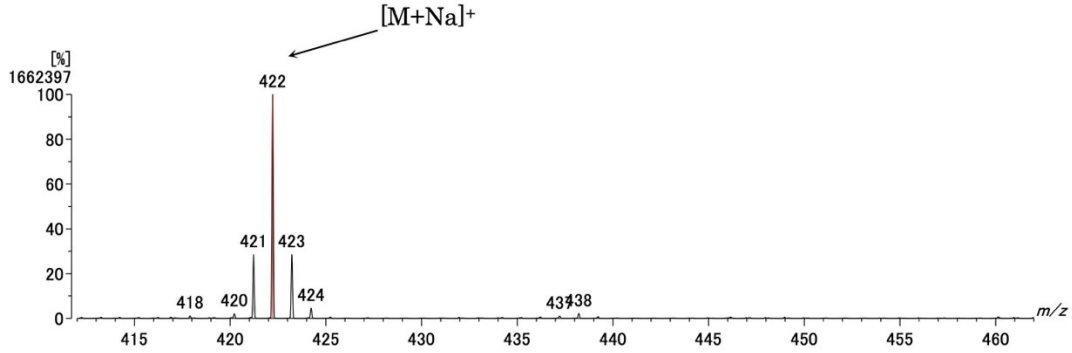

Fig. S8. FAB mass spectrum of **BHBA-p**–**MPBA**.

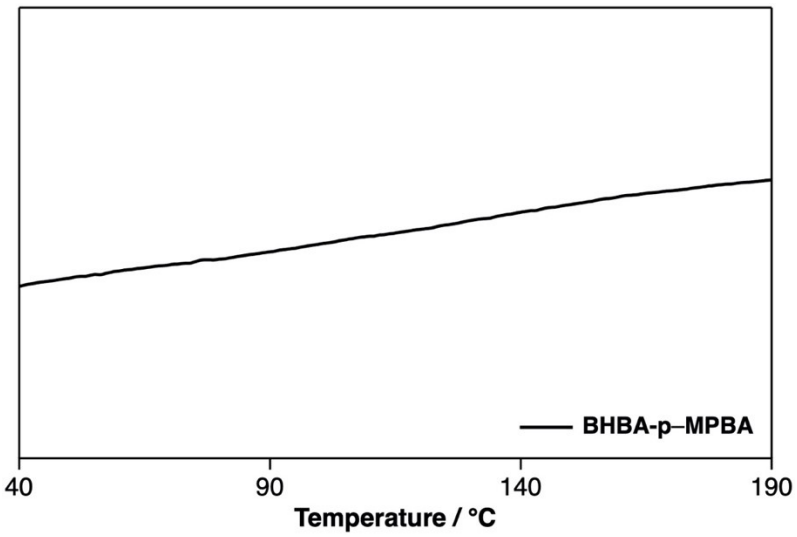

Fig. S9. DSC profile of **BHBA-p**–**MPBA** at a heating rate of 10 °C/min.

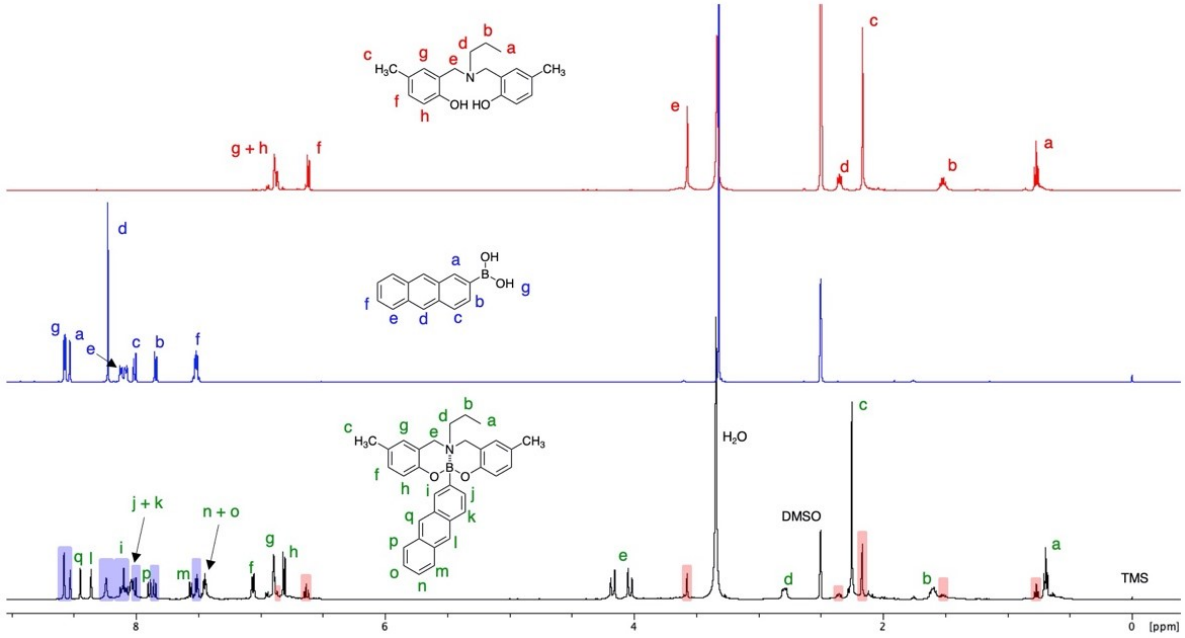

Fig. S10. [1]H NMR spectra of DOAB formed with equimolar **BHBA-p** and **2-AnBA** (black), **2-AnBA** (blue), and **BHBA-p** (red) (DMSO-d_6, 500 MHz). In the bottom spectrum, signals corresponding to the **BHBA-p** and **2-AnBA** are highlighted in red and blue, respectively.

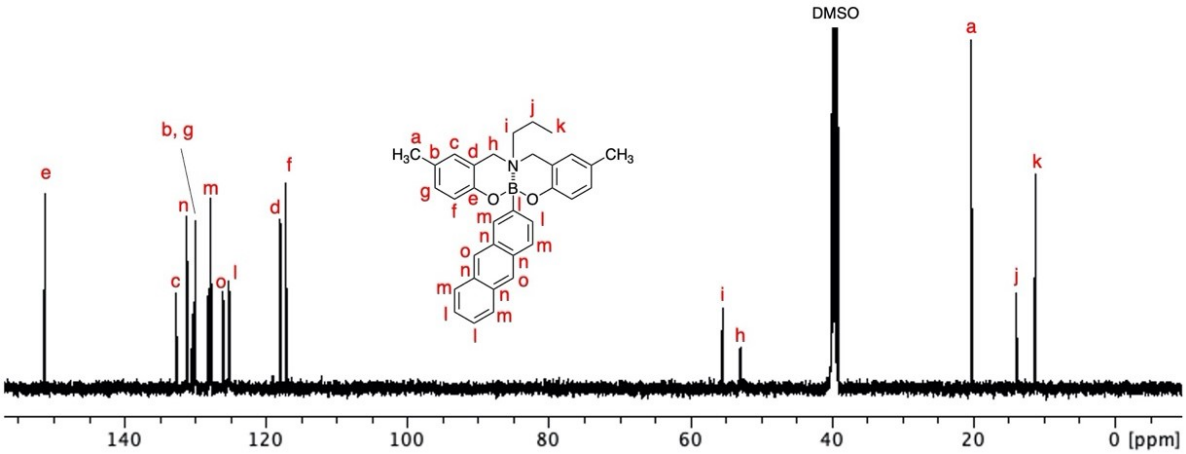

Fig. S11. [13]C NMR spectra of **BHBA-p**–**2-AnBA** (DMSO-d_6, 125 MHz).

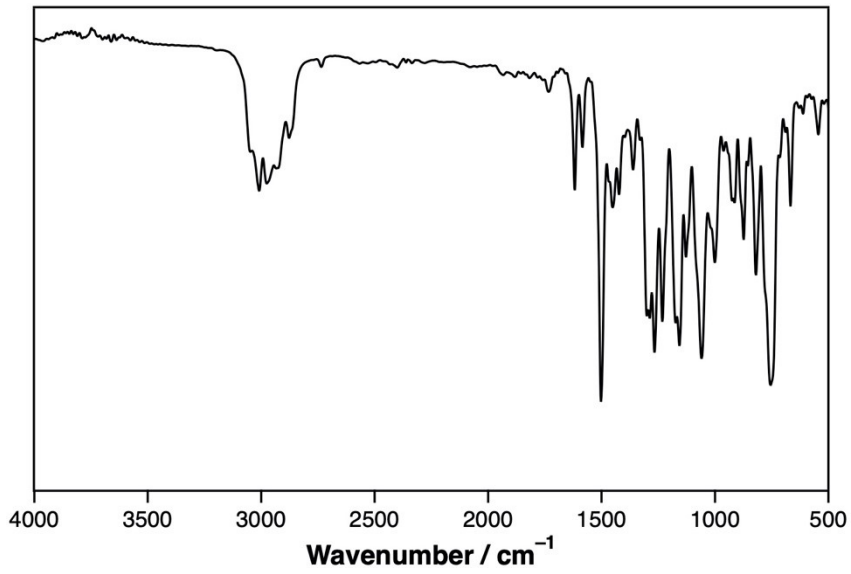

Fig. S12. FT-IR spectrum of **BHBA-p**–**2-AnBA** (NaCl).

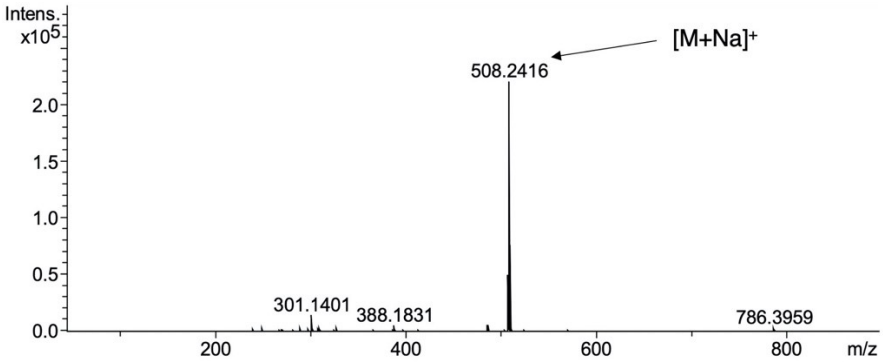

Fig. S13. ESI mass spectrum of **BHBA-p**–**2-AnBA**.

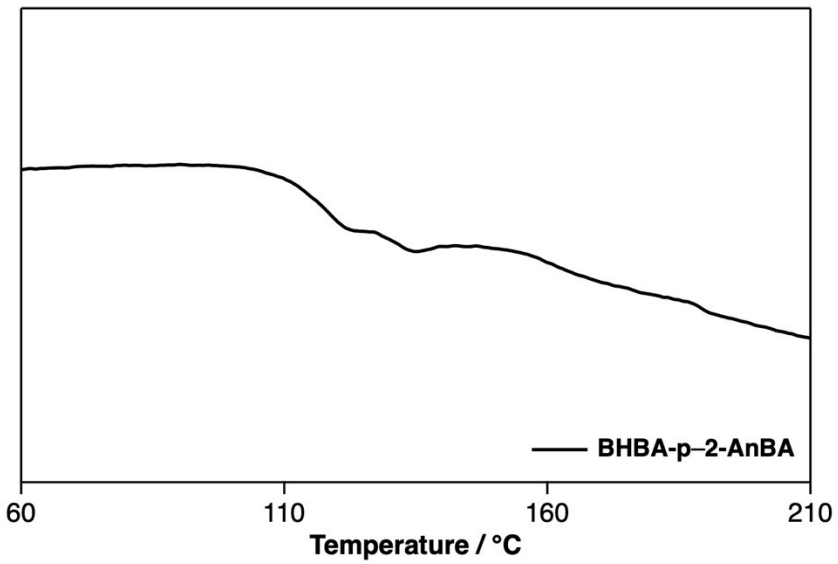

Fig. S14. DSC profile of **BHBA-p**–**2-AnBA** at a heating rate of 10 °C/min.

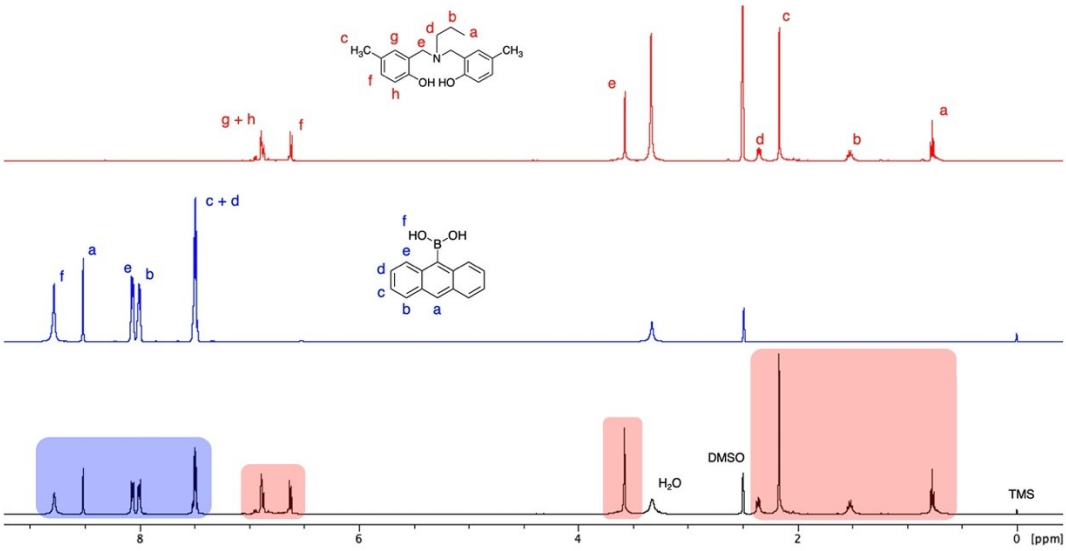

Fig. S15. ^{1}H NMR spectra of the mixture of equimolar **BHBA-p** and **9-AnBA** (black), **9-AnBA** (blue), and **BHBA-p** (red) (DMSO-d_6, 500 MHz). In the bottom spectrum, signals corresponding to the **BHBA-p** and **9-AnBA** are highlighted in red and blue, respectively.

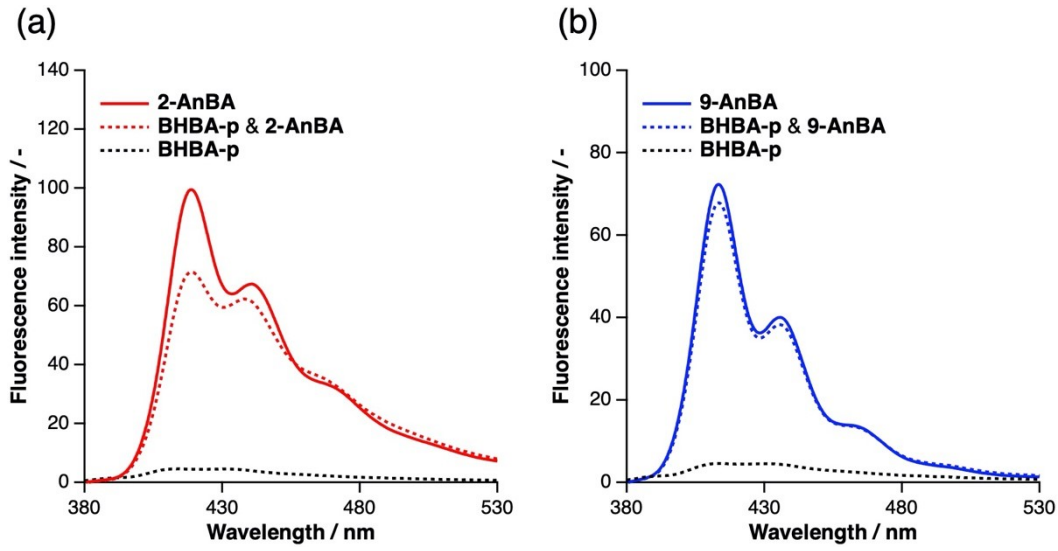

Fig. S16. Fluorescence emission spectra of **BHBA-p** mixed with the eqmiuimolar amount of an anthraceneboronic acid, an anthraceneboronic acid, and **BHBA-p** in DMSO at room temperature. Sample concentration was 5.6 × 10^{-3} M for all measurements. λ_{ex} = 365 nm. (a) Spectra of samples using **2-AnBA**. λ_{em} shifted from 441 nm to 438 nm after addition of **BHBA-p** to **2-AnBA**. (b) Spectra of samples using **9-AnBA**. λ_{em} remained at 413 nm and 436 nm.

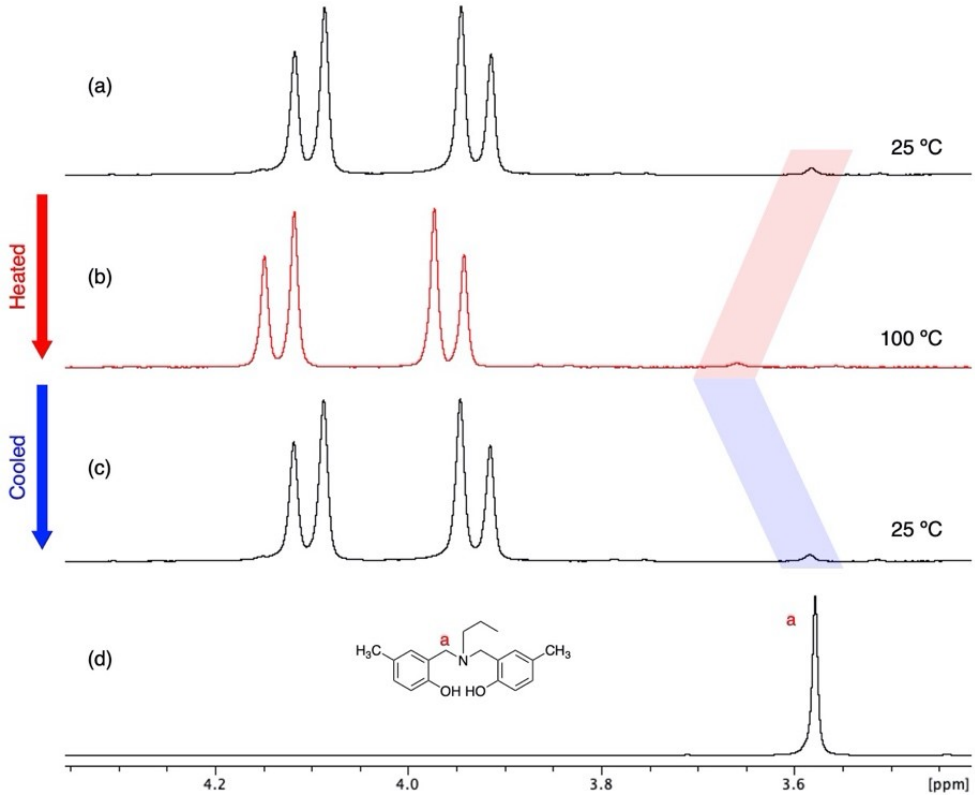

Fig. S17. Variable temperature ^{1}H NMR spectra of **BHBA-p**–**MPBA** (a) after heating at 100 °C for 384 h and then ^{1}H NMR measurement was taken at 25 °C within 30 min, (b) sample taken at 25 °C was then heated to 100 °C within 30 min and ^{1}H NMR measurement was taken at 100 °C, (c) sample taken at 100 °C was then cooled to 25 °C and ^{1}H NMR measurement was taken at 25 °C, (d) spectrum of **BHBA-p** at 25 °C (DMSO-d_6, 500 MHz). Note; The binding constants calculated from peak intensity in a, b, and c were identical, supporting that the short-term change in temperature for temporary ^{1}H NMR measurement does not affect the decomposition reaction.

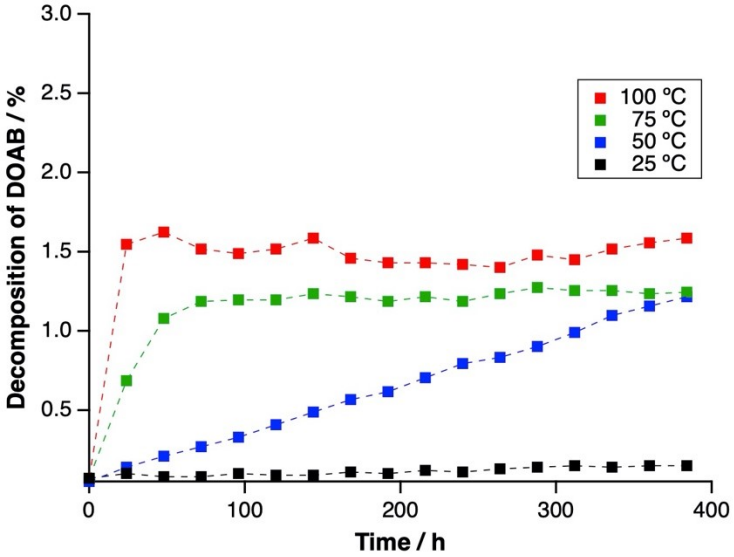

Fig. S18. Decomposition of DOAB (**BHBA-p**–**MPBA**) as a function of heating time at each temperature. Decomposition of DOAB was determined by ^{1}H NMR (DMSO-d_6, 500 MHz).

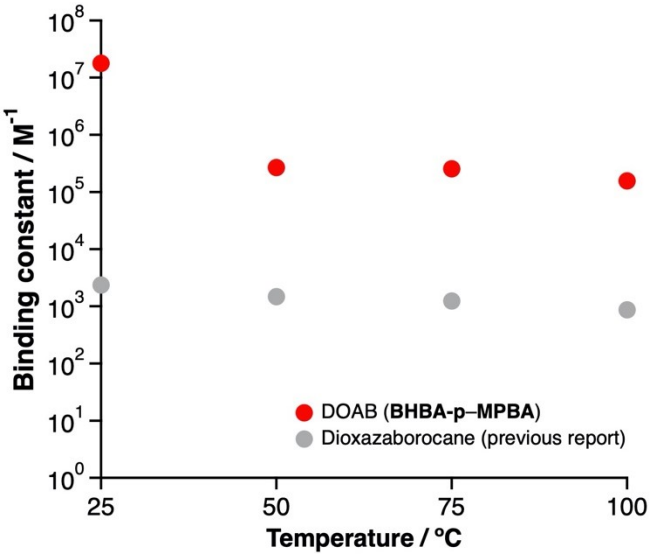

Fig. S19. Binding constant of DOAB (**BHBA-p**–**MPBA**) (red), and previously reported dioxazaborocane formed with diethanolamine and **MPBA**[6] (gray) at 25–100 °C in DMSO-d_6.

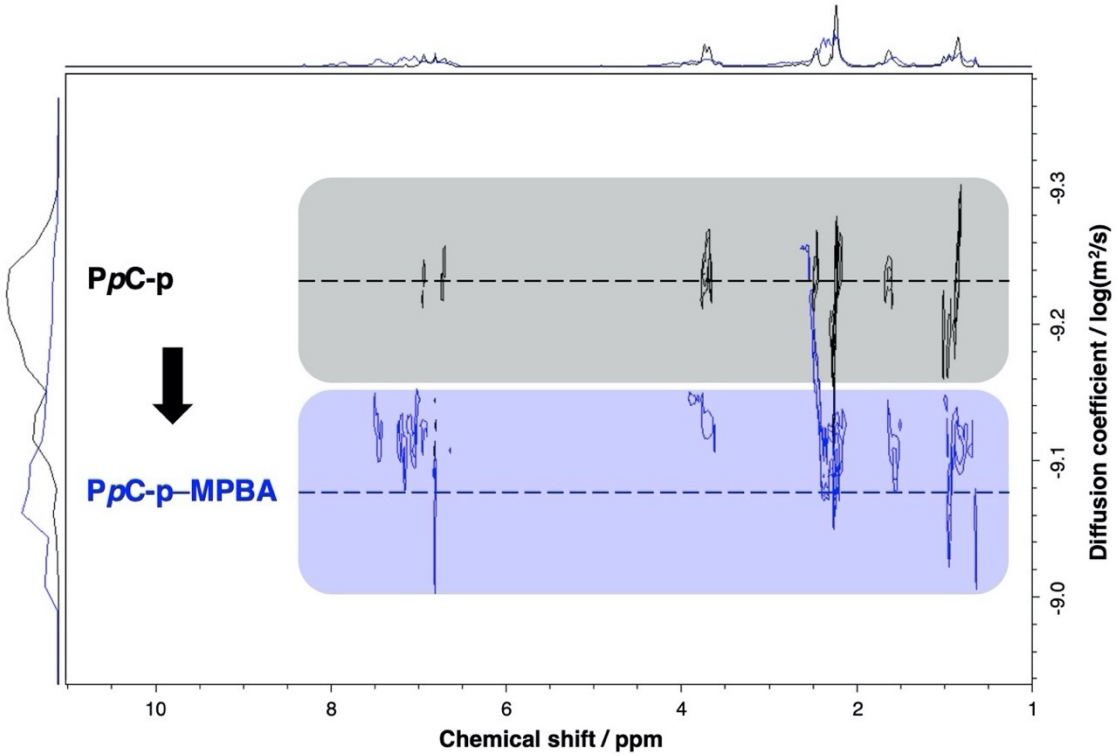

Fig. S20. Stacked DOSY spectra of **P*p*C-p** (black) and **P*p*C-p–MPBA** (blue) in $CDCl_3$.

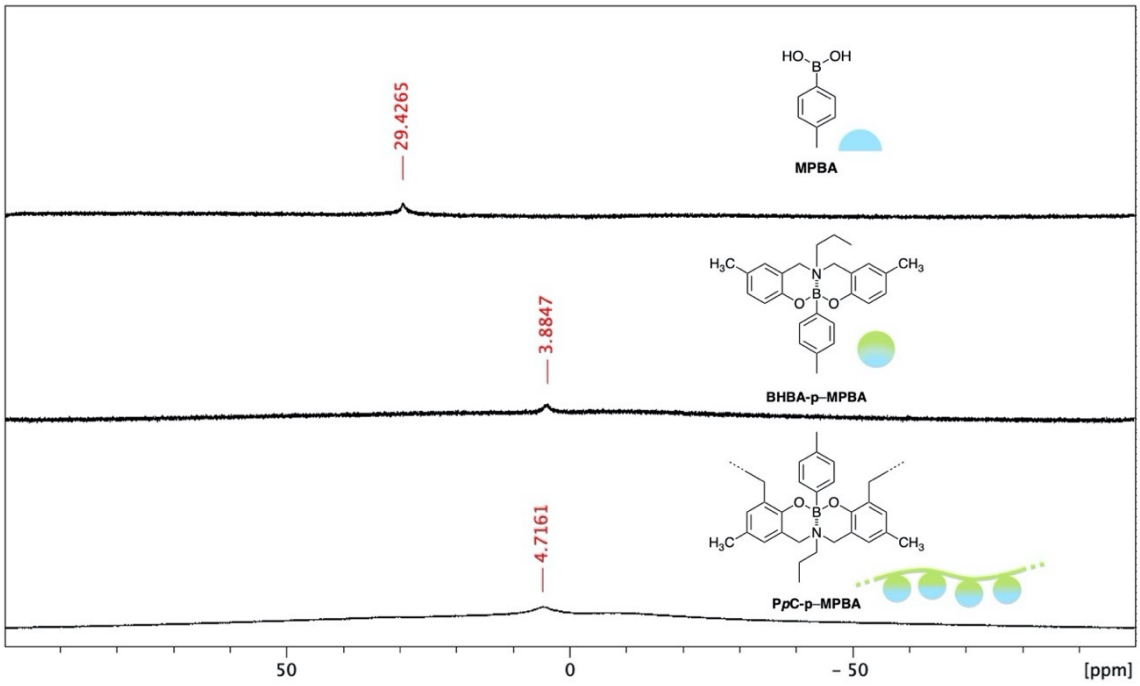

Fig. S21. ^{11}B NMR spectra of **MPBA** (top), **BHBA-p–MPBA** (middle), **P*p*C-p–MPBA** (bottom). The reference signal of BF_3OEt_2 at δ = 0.00 ppm is not shown.

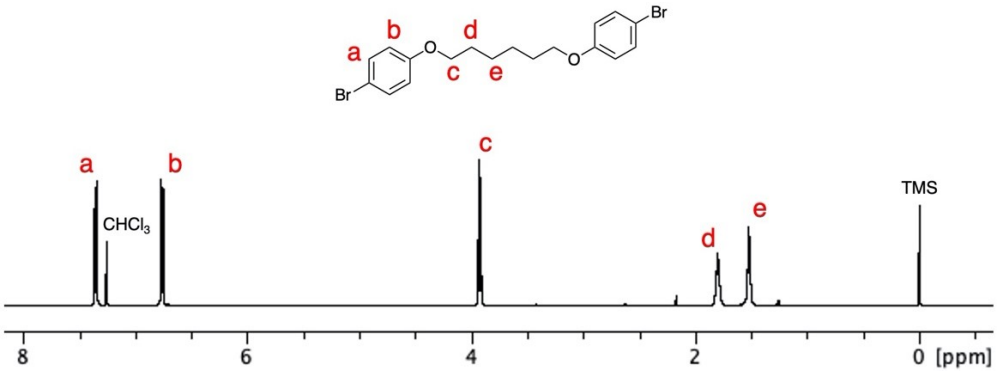

Fig. S22. ^{1}H NMR spectrum of **1** ($CDCl_3$, 500 MHz).

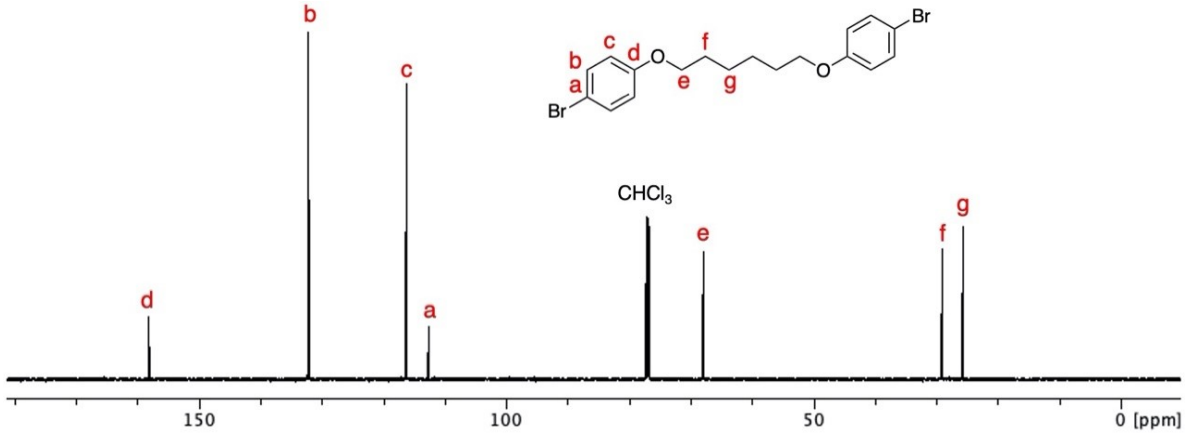

Fig. S23. ^{13}C NMR spectrum of **1** ($CDCl_3$, 125 MHz).

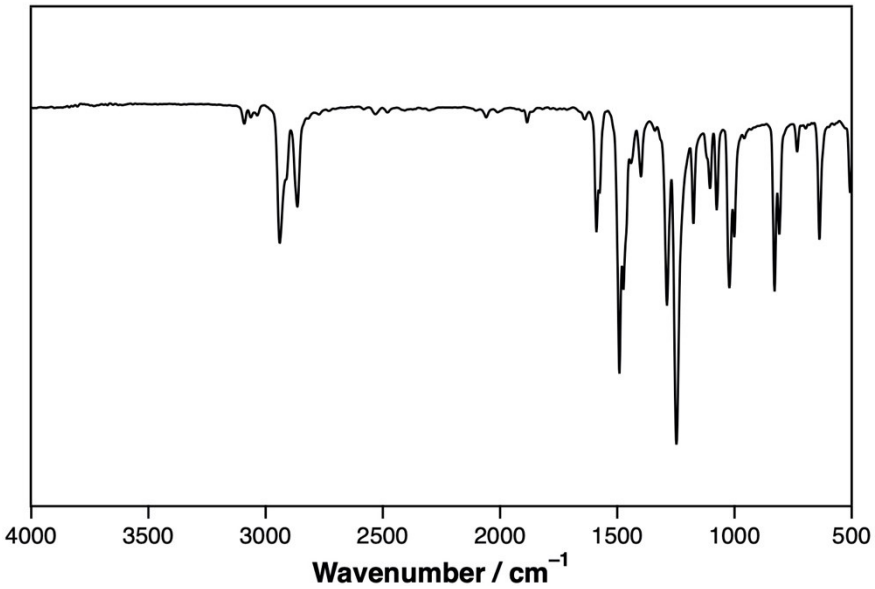

Fig. S24. FT-IR spectrum of **1** (KBr).

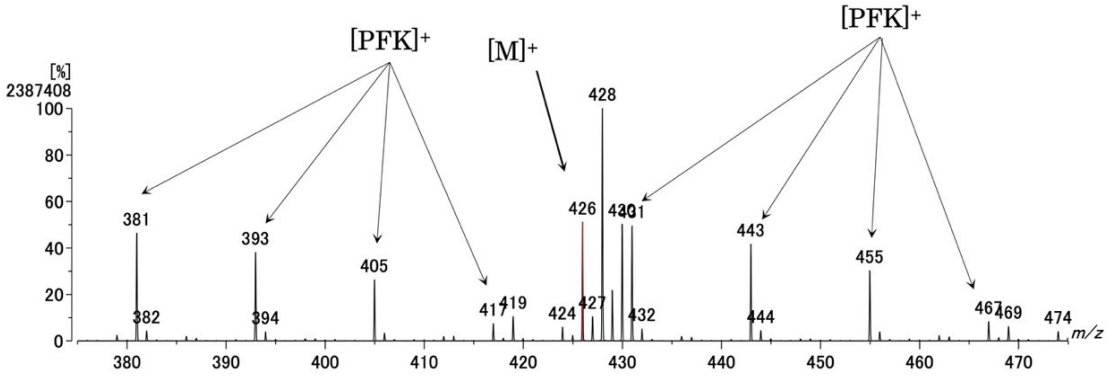

Fig. S25. EI mass spectrum of **1**.

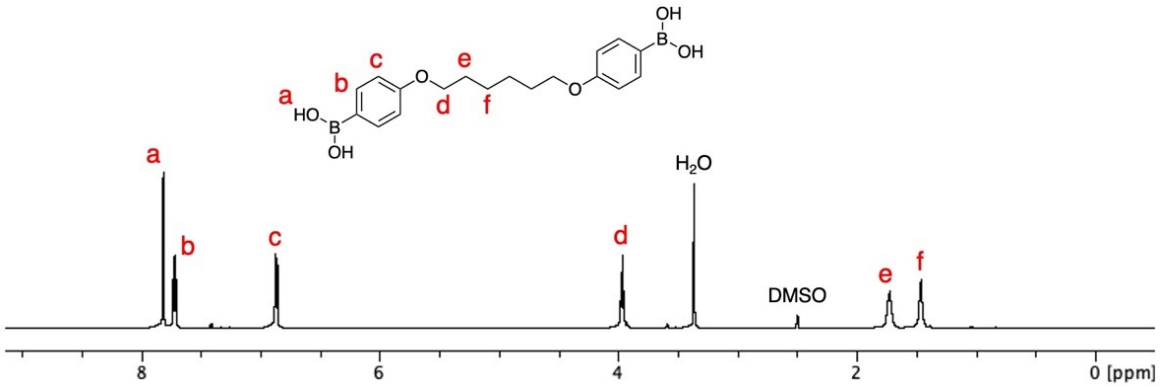

Fig. S26. ^{1}H NMR spectrum of **diBA** ($CDCl_3$, 500 MHz).

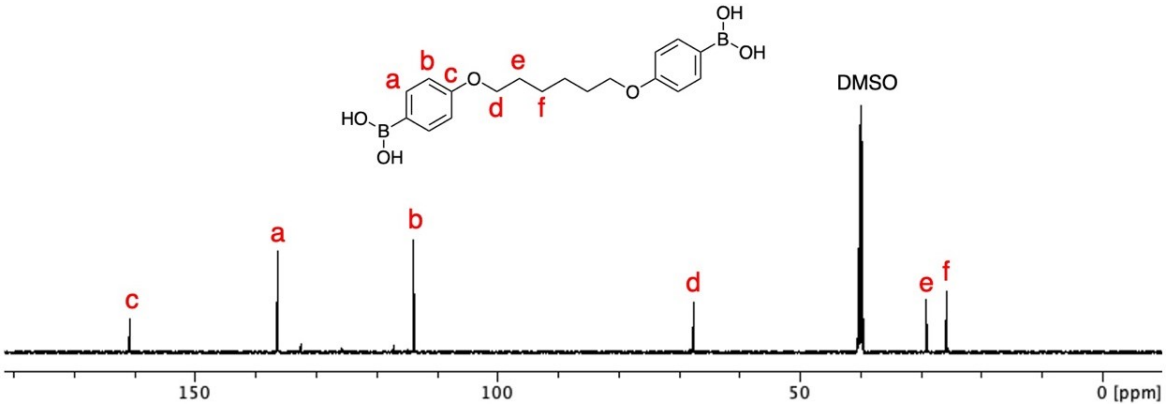

Fig. S27. ^{13}C NMR spectrum of **diBA** (DMSO-d_6, 125 MHz). C–B was not detected.

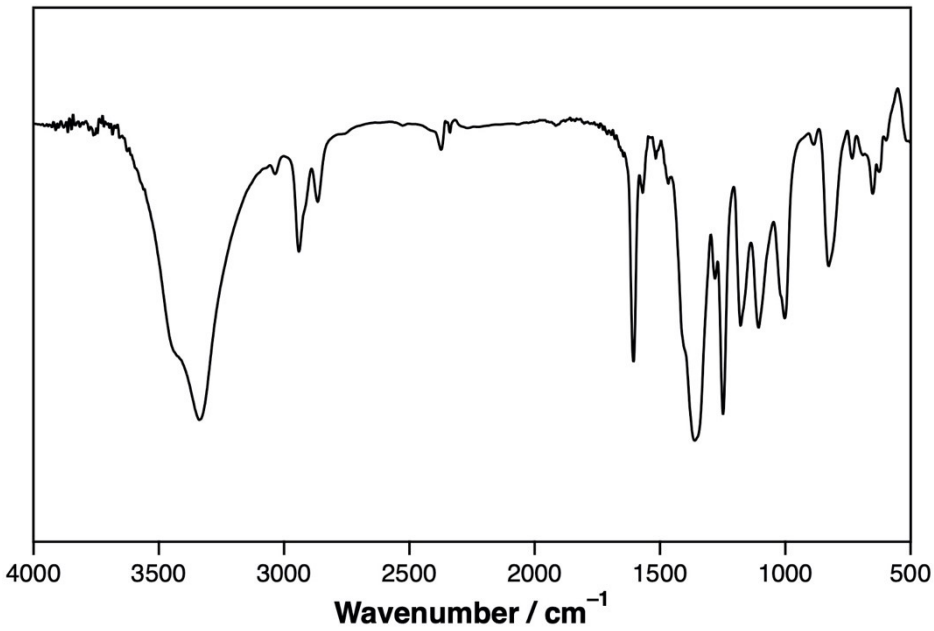

Fig. S28. FT-IR spectrum of **diBA** (KBr).

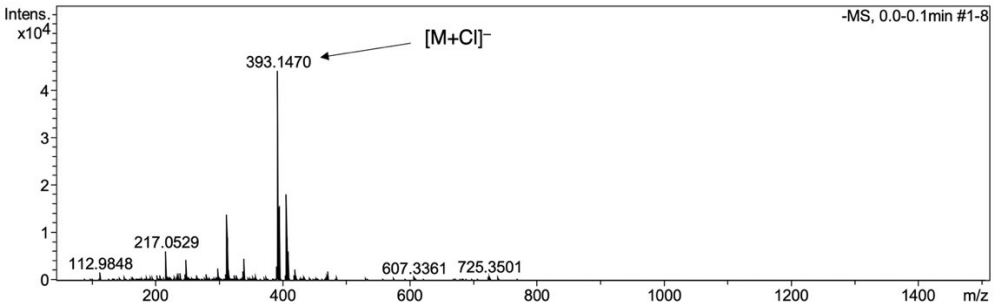

Fig. S29. ESI mass spectrum of **diBA**.

Fig. S30. A photograph of **PB-p**.

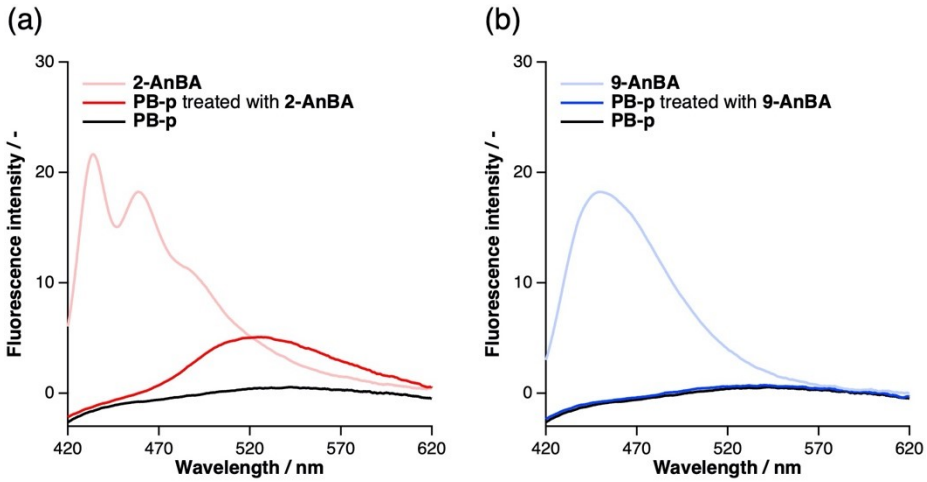

Fig. S31. Solid-state fluorescence emission spectra of an anthraceneboronic acid, **PB-p** treated with an anthraceneboronic acid, and **PB-p** at room temperature. λ_{ex} = 365 nm. (a) Spectra of samples using **2-AnBA**. λ_{em} of treated **PB-p** was 526 nm. (b) Spectra of samples using **9-AnBA**.

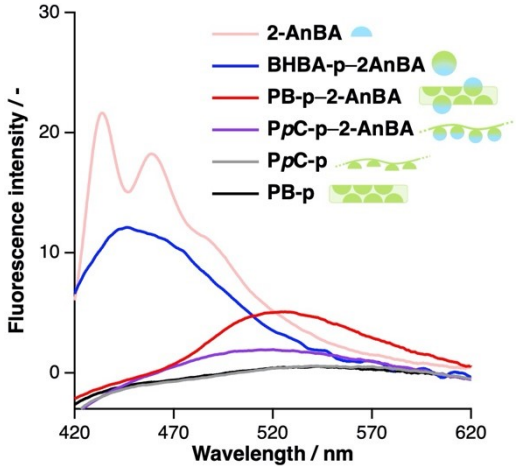

Fig. S32. Solid-state fluorescence emission spectra of **2-AnBA** (pink), **BHBA-p–2AnBA** (blue), **PB-p–2-AnBA** (red), **P*p*C-p–2-AnBA** (purple), **P*p*C-p** (gray), and **PB-p** (black) at room temperature. λex = 365 nm.

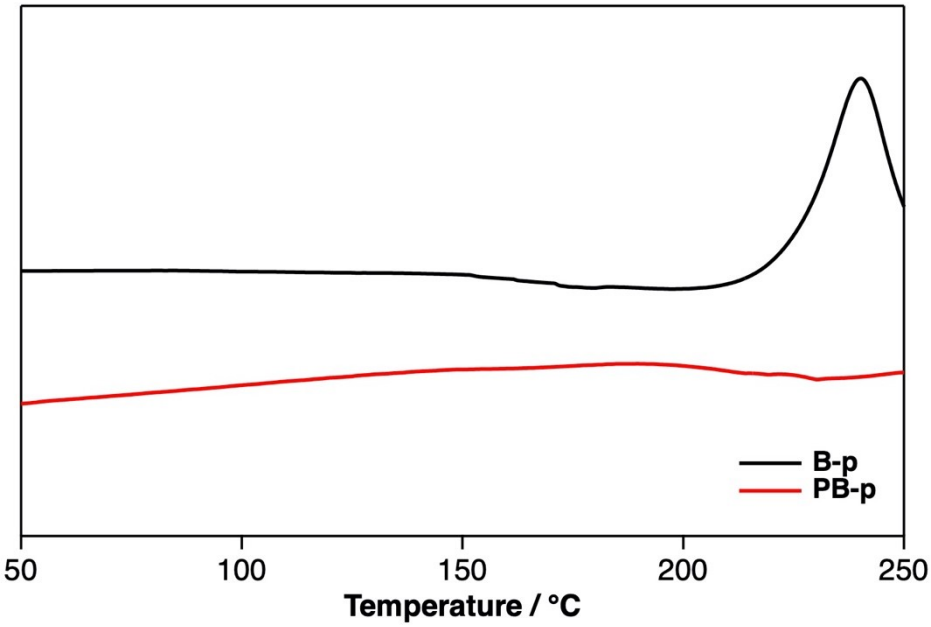

Fig. S33. DSC profiles of **B-p** (black) and **PB-p** which is prepared under the following condition (red): 140 °C, 2 h; 160 °C, 2 h; 180 °C, 2 h; 200 °C, 15 h. DSC measurements were carried out at a heating rate of 10 °C/min.

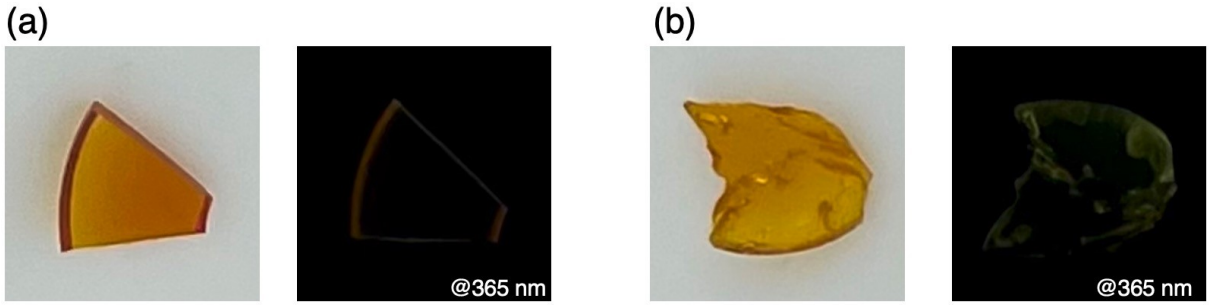

Fig. S34. Photographs under irradiation from visible (left) and UV light (right) of (a) fully cured **PB-p** and (b) fully cured **PB-p** treated with **2-AnBA** in THF at 50 °C for 48 h.

References

1 (a) S. Chirachanchai, A. Laobuthee and S. Phongtamrug, *J. Heterocycl. Chem.*, 2009, **46**, 714–721. (b) K. Hemvichian, A. Laobuthee, S. Chirachanchai and H. Ishida, *Polym. Degrad. Stab.*, 2002, **76**, 1–15.

2 H. Oie, A. Sudo and T. Endo, *J. Polym. Sci. Part A Polym. Chem.*, 2010, **48**, 5357–5363.

3 X. Zhang, S. Wang, Z. Jiang, Y. Li and X. Jing, *J. Am. Chem. Soc.*, 2020, **142**, 21852–21860.

4 M. B. Nielsen, J. O. Jeppesen, J. Laut, C. Lomholt, D. Damgaard, J. P. Jacobsen, J. Becher and J. F. Stoddart, *J. Org. Chem.*, 2001, **66**, 3559–3563.

5 S. M. Jansze, M. D. Wise, A. V. Vologzhanina, R. Scopelliti and K. Severin, *Chem. Sci.*, 2017, **8**, 1901–1908.

6 Y. Ito, J. Kida, D. Aoki and H. Otsuka, *Chem. Commun.*, 2018, **54**, 12930–12933.